

Performance evaluation of static and kinematic precise point positioning in forest-obstructed environments

Youpeng Zhang and Jincheng Liu*

College of Natural Resources and Environment, Northwest A&F University, Yangling 712100, China

* Correspondence: jinchengl@nwfau.edu.cn (Liu J)

Abstract

Precise Point Positioning (PPP) enables high-accuracy GNSS positioning without reference stations, but remains highly vulnerable to signal obstruction in forested environments. This study presents a long-term quantitative investigation of static and kinematic PPP performance under forest canopy conditions, using multi-GNSS observations collected from DOY 078 to 195 in 2023, with open-sky observations serving as reference baselines. Positioning accuracy and convergence behavior were evaluated against double-difference solutions using mean deviation, standard deviation, and RMSE, together with analyses of satellite visibility and PDOP. The results demonstrate pronounced differences in PPP performance under forest canopy conditions. Static PPP suffers pronounced performance degradation under canopy obstruction, with convergence times exceeding 30–40 min and vertical errors increasing to the meter level, particularly under dense vegetation. In contrast, kinematic PPP demonstrates greater robustness in forested scenarios, maintaining sub-meter accuracy and more stable convergence. A nonlinear relationship between canopy density and PPP performance is identified, indicating a critical canopy-closure threshold beyond which static solutions frequently fail to converge reliably. This behavior is primarily attributed to motion-induced geometric diversity and filtering continuity. These findings provide quantitative evidence for selecting appropriate PPP strategies in forested environments and offer practical guidance for GNSS applications in forestry, agriculture, and environmental monitoring.

Citation: Zhang Y, Liu J. 2026. Performance evaluation of static and kinematic precise point positioning in forest-obstructed environments. *Smart Forestry* 1: e005 <https://doi.org/10.48130/smartfor-0026-0002>

Introduction

With the rapid advancement of Global Navigation Satellite System (GNSS) technology, the integration of multiple satellite constellations—including the Global Positioning System (GPS), the BeiDou Navigation Satellite System (BDS), GLONASS, and the Galileo system—has significantly enhanced global positioning capability and availability^[1,2]. Together with the widespread availability of high-precision satellite orbit and clock products, Precise Point Positioning (PPP) has emerged as a powerful positioning technique capable of achieving centimeter- to decimeter-level accuracy without reliance on local reference station networks^[3,4]. Owing to its infrastructure independence and global applicability, PPP has been widely adopted in scientific research and engineering practice, particularly in remote, rural, and infrastructure-limited regions^[5–7]. PPP achieves high positioning accuracy by integrating precise satellite orbits and clocks, earth orientation parameters, and advanced observation and stochastic models^[8–10]. Continuous improvements in multi-constellation GNSS systems, precise products and processing strategies have further enhanced the robustness and applicability of PPP across diverse operational scenarios^[11,12]. Nevertheless, the positioning performance of PPP remains highly sensitive to observational environment quality, particularly in complex and obstructed scenarios, among which forested environments represent one of the most challenging and least understood application cases for PPP^[13–16].

Forested environments represent one of the most challenging scenarios for GNSS-based positioning. The heterogeneous structure of forest canopies, consisting of trunks, branches, and foliage, leads to complex signal propagation phenomena, including attenuation, diffraction, and severe multipath effects^[17,18]. Numerous studies have demonstrated that forest canopy obstruction can significantly degrade GNSS positioning accuracy by reducing satellite visibility and increasing observational noise^[19]. The impact of vegetation on

GNSS signals is strongly dependent on forest type and structure: coniferous forests, for instance, often exert a more pronounced adverse effect than broad-leaved forests due to denser canopies and vertically oriented trunks^[20,21]. These characteristics highlight the importance of explicitly accounting for vegetation structure and density when evaluating PPP performance in forested environments. These characteristics make forest environments a critical testbed for evaluating the practical limits of PPP positioning performance. Most existing investigations of PPP performance under forest canopy conditions have primarily focused on static observation modes^[3,10]. In static PPP, receiver coordinates are treated as constant parameters, allowing long-term observation accumulation and temporal averaging to suppress random errors and enhance solution stability. In contrast, kinematic PPP estimates receiver positions epoch by epoch, relying more heavily on observation continuity and instantaneous satellite geometry^[22,23]. These two modes differ fundamentally in their estimation strategies and handling of temporal information, which may lead to contrasting performance under challenging observation environments^[24,25].

Under forest canopy conditions, these methodological differences are expected to result in substantially different positioning behaviors between static and kinematic PPP. Previous studies indicate that motion-induced geometric diversity associated with receiver movement may partially enhance the robustness of kinematic PPP under weak-signal conditions^[22,24]. However, it remains unclear whether such potential benefits can effectively compensate for vegetation-induced signal degradation, particularly under increasing canopy density. Consequently, the key limitation in current research lies in the lack of a mechanism-oriented understanding of how static and kinematic PPP respond differently to vegetation-induced signal obstruction and multipath interference^[26,27]. In forested environments, PPP performance is influenced not only by spatial variations in canopy density but also by temporal canopy dynamics and operational conditions. Seasonal

changes in canopy structure introduce pronounced temporal variability in GNSS signal propagation, altering signal attenuation characteristics and multipath behavior, and leading to time-dependent variations in PPP accuracy and convergence performance^[28]. Few long-term, systematic studies have investigated how seasonal canopy dynamics affect PPP performance^[29]. Beyond vegetation-related factors, operational conditions—including receiver type, antenna design, installation height, and handling practices—also play a critical role in determining GNSS positioning performance under forest canopies^[30–35]. These factors, together with satellite constellation geometry, elevation angle thresholds, and terrain characteristics, jointly influence positioning accuracy and solution stability in complex forest environments^[36,37].

Based on the above considerations, this study aims to go beyond conventional performance comparisons by systematically investigating the mechanisms governing PPP accuracy degradation and convergence behavior under forest canopy conditions. Open-sky scenarios are used as reference baselines, with particular emphasis on the contrasting responses of static and kinematic PPP to vegetation density and seasonal canopy dynamics. Specifically, this study addresses the following research questions: (1) How do static and kinematic PPP differ in positioning accuracy, convergence behavior, and robustness under varying degrees of forest canopy obstruction? (2) To what extent can motion-induced geometric diversity in kinematic PPP mitigate canopy-induced signal degradation compared with static PPP? (3) How does observation duration interact with canopy density to influence PPP convergence characteristics?

To address these questions, multi-constellation GNSS observation data were collected using M68 receivers provided by Beijing BDStar Navigation Co., Ltd, covering Day of Year (DOY) 078 to 195 in 2023. Both static and kinematic experiments were conducted under open-sky conditions and varying degrees of canopy closure. Advanced multi-frequency PPP processing strategies were applied, with independent reference solutions used for validation. By systematically analyzing positioning accuracy, convergence characteristics, and sensitivity to vegetation density and seasonal variation, this study seeks to provide mechanism-oriented insights and practical guidance for PPP deployment in forested environments, supporting applications in forestry surveying and related fields.

Materials and methods

Data description

To support a focused and reproducible evaluation of PPP performance under forest canopy conditions, GNSS data was collected using an M68 receiver manufactured by Beijing BDStar Navigation Technology Co., Ltd. The M68 receiver is based on a Linux operating system and a Qualcomm MDM9628 Cortex-A7 platform, providing sufficient computational capability for multi-frequency and multi-constellation GNSS processing. The integrated high-precision GNSS module supports full-constellation and full-frequency signal tracking, including BDS (B1/B2/B3), GPS (L1/L2/L5), GLONASS (L1/L2), Galileo (E1/E5a/E5b), as well as SBAS (L1) and QZSS (L1/L2/L5). In addition, the receiver is equipped with an embedded high-precision inertial measurement unit (IMU), enabling real-time tilt compensation during kinematic observations. Data transmission and remote communication are supported through a Linux-based 4G cellular module compatible with major network standards. A compact integrated antenna combining GNSS, 4G, WiFi, and Bluetooth functionalities was used to ensure stable signal reception under field conditions. These specifications ensure compatibility with high-precision PPP processing and facilitate reproducibility of the experimental setup. The observation campaign spanned from

Day of Year (DOY) 078 to 195 in 2023, with data collection sessions conducted at approximately weekly intervals. This long-term and periodic sampling strategy was designed to capture variations in canopy density and seasonal vegetation dynamics, which are known to strongly influence GNSS signal propagation in forested environments, while maintaining a consistent experimental configuration.

During each observation session, GNSS data were recorded at a sampling interval of 1 s to preserve short-term signal fluctuations and satellite visibility changes that are particularly critical for kinematic PPP under canopy obstruction. A satellite elevation cutoff angle of 10° was applied to mitigate severe low-elevation multipath effects while retaining sufficient satellite availability in forested conditions. Owing to the large number of observation cycles, the dataset acquired on DOY 085 was selected as a representative example to illustrate the kinematic data acquisition trajectories, whereas the complete dataset was retained for subsequent statistical and performance analyses.

The experimental design primarily targeted forest-obstructed scenarios, with open-sky observations introduced as a reference baseline to isolate and quantify canopy-induced effects on PPP performance. Accordingly, the dataset comprises both static and kinematic GNSS observations collected under forest canopy conditions, supplemented by corresponding open-sky measurements conducted using identical equipment and processing strategies. The forest-obstructed kinematic experiments were carried out in an artificial beech plantation located at Northwest A&F University, Shaanxi Province, China (34°15'45" N, 108°03'34" E). This site provides a controlled yet representative forest environment characterized by dense foliage and complex signal obstruction, making it suitable for evaluating PPP performance in typical forestry and ecological monitoring scenarios. For reference purposes, open-sky observations were conducted in a nearby unobstructed field north of the campus (34°17'46" N, 108°02'59" E).

Although direct measurements of leaf area index (LAI) or canopy closure were not available in this study, satellite visibility and PDOP were adopted as indirect proxy variables to characterize canopy density. Previous GNSS studies in forested environments have demonstrated strong correlations between vegetation density, satellite visibility, PDOP variation, and positioning performance. In the artificial beech plantation investigated here, the canopy is characterized by broad leaves and relatively continuous crown structures, with pronounced seasonal foliage development. Under such conditions, long-term variations in satellite availability and PDOP provide an effective surrogate for assessing relative changes in canopy obstruction.

During kinematic observations, the GNSS receiver was mounted on a vehicle and operated along predefined and repeatable trajectories to ensure consistent motion characteristics across sessions. Representative kinematic trajectories under forest canopy and open-sky conditions are shown in Fig. 1, which serves to document the experimental configuration and movement patterns rather than to assess positioning accuracy.

To establish reliable reference coordinates for positioning accuracy evaluation, a continuously operating GNSS reference station was installed on the rooftop of the College of Forestry at Northwest A&F University. This reference station provided stable and continuous observations throughout the entire campaign, enabling the generation of high-accuracy reference solutions for the quantitative assessment of PPP-derived positions. The availability of a fixed reference station ensures that positioning errors can be evaluated consistently across different canopy conditions and positioning modes.

Given the extended duration of the observation campaign, a staged sampling strategy was adopted to ensure temporal representativeness while minimizing data redundancy. Specifically,

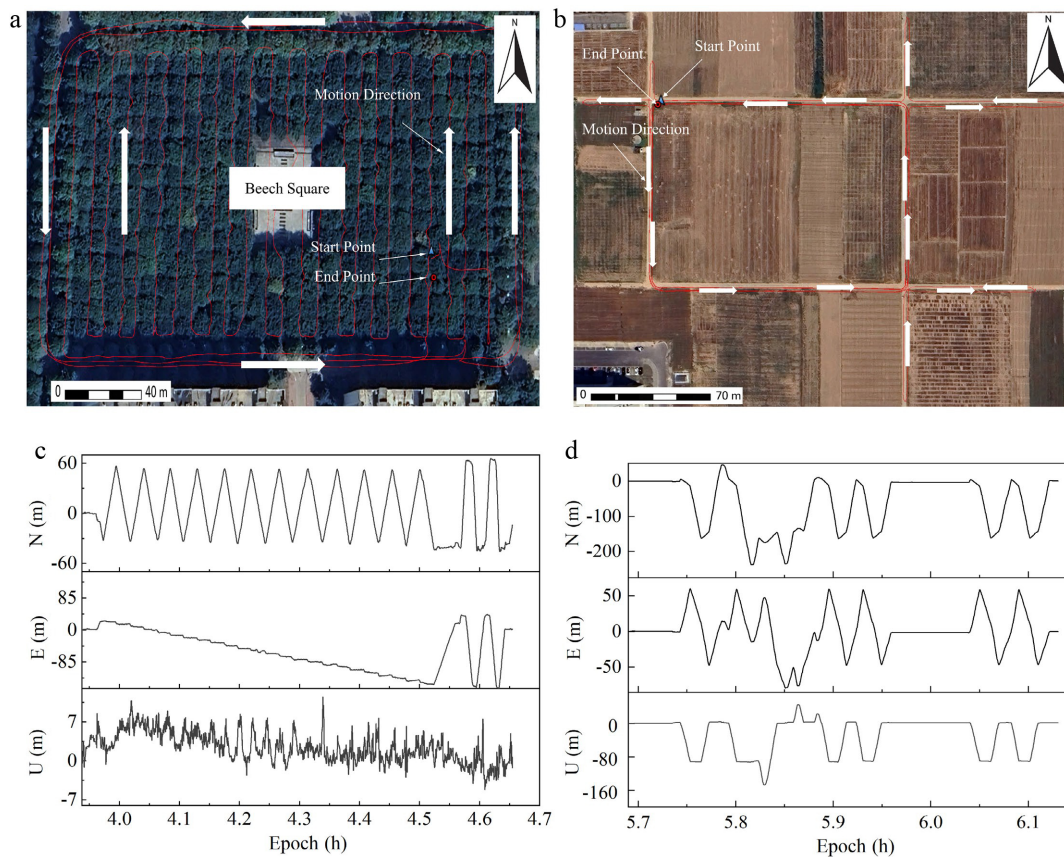


Fig. 1 Comparison of GNSS trajectories and coordinate components in different environments. (a) Forest trajectories, (b) open-sky trajectories, (c) forest, and (d) open-sky N/E/U components in the barycentric coordinate system.

two representative observation sessions were selected from each of the early, middle, and late phases of the experiment to capture variations in satellite geometry and environmental conditions associated with seasonal canopy evolution. All datasets were collected using integrated multi-constellation GNSS observations, including GPS, GLONASS, BDS, and Galileo.

Under forest-obstructed conditions, satellite visibility exhibited pronounced reductions and strong temporal variability due to canopy-induced signal attenuation and blockage. Both static and kinematic observations were characterized by frequent fluctuations in the number of tracked satellites and corresponding variations in Position Dilution of Precision (PDOP), reflecting degraded and unstable satellite geometry beneath the forest canopy. These features represent typical GNSS observation conditions encountered in forested environments, and provide a realistic basis for evaluating PPP performance under canopy obstruction.

For reference purposes, open-sky observations were conducted under identical experimental settings. In these baseline scenarios, satellite availability remained high, and observation geometry was generally stable, with consistently low PDOP values for both static and kinematic observations. This reference dataset enables isolation of canopy-induced effects by comparison with forest-obstructed observations. Statistical summaries of satellite availability and PDOP variations under both scenarios are presented in Figs 2 and 3.

To provide a quantitative overview of canopy-induced signal degradation over time, satellite availability and PDOP statistics were summarized for the early (DOY 078–100), middle (DOY 101–140), and late (DOY 141–195) observation phases. Results show a progressive decrease in the mean number of visible satellites accompanied by increased PDOP variability from early to late phases, reflecting

the gradual densification of forest canopy during the growing season. These trends support the use of satellite visibility and PDOP as effective indicators of canopy density evolution.

Data processing models

PPP performance under complex environmental conditions was evaluated using GNSS observations collected over a 117-d period from DOY 078 to 195 in 2023. High-precision products provided by the German Research Centre for Geosciences (GFZ) were employed throughout the data processing, including precise satellite orbit and clock corrections, earth rotation parameters (ERP), and observable-specific signal bias (OSB) corrections. The use of consistent, high-quality external products ensured the temporal stability and reliability of the positioning solutions across the entire experimental campaign. It should be noted that the relative offset between the PPP receiver and the reference station does not affect the evaluation results, as all PPP solutions are assessed against double-difference reference coordinates expressed in the same ITRF14 reference frame, and corrected using identical antenna phase center models.

Both static and kinematic PPP solutions were processed using an undifferenced observation model, which represents the standard formulation for high-precision PPP applications. Although sharing the same fundamental observation equations, static and kinematic PPP differ in their parameter estimation strategies. In static PPP, receiver coordinates are treated as constant unknowns, allowing long-term observation accumulation to enhance noise averaging and ambiguity convergence. In contrast, kinematic PPP estimates receiver positions epoch by epoch, making the solution more sensitive to instantaneous satellite geometry variations, signal interruptions, and multipath effects, particularly under obstructed conditions.

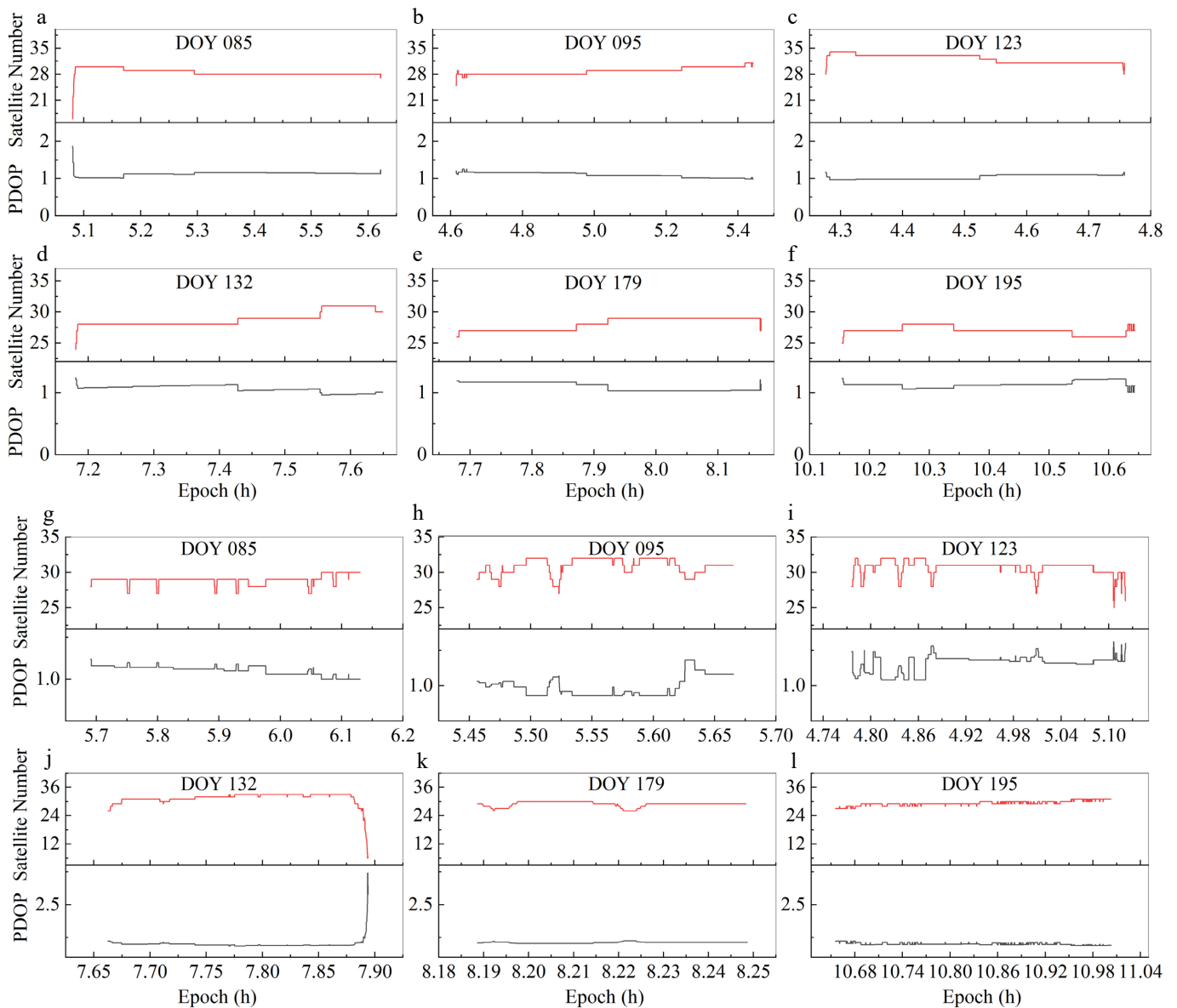


Fig. 2 Performance of satellite availability and PDOP in open-sky scenarios across different observation days. (a)–(f) Static mode for DOY 085, 095, 123, 132, 179, and 195, respectively. (g)–(l) Kinematic mode for the corresponding DOY sequence.

To ensure objective, consistent, and comparable accuracy assessment, double-difference (DD) positioning solutions were adopted as reference truth values^[6]. The DD approach is widely recognized for its effectiveness in eliminating common-mode errors, such as satellite orbit and clock biases, and thus provides a reliable benchmark for evaluating PPP-derived positions. PPP performance was quantitatively assessed by comparing PPP solutions with the DD reference coordinates.

The detailed PPP processing strategies, applied correction models, and evaluation metrics are summarized in [Table 1](#), providing a transparent and reproducible framework for the comparative analysis of static and kinematic PPP performance under different environmental scenarios.

Statistical analysis

To quantitatively evaluate the performance of PPP under different observation modes and environmental conditions, a unified statistical analysis framework was adopted for all datasets. PPP-derived position solutions were assessed by comparison with

high-precision DD reference coordinates expressed in the same ITRF14 reference frame, and corrected using identical antenna phase center models.

Positioning errors were calculated separately for the east (E), north (N), and up (U) components. Three statistical indicators were used to characterize positioning performance: mean deviation (Mean), standard deviation (STD), and root mean square error (RMSE). The mean deviation reflects systematic bias, the standard deviation represents solution dispersion, and the RMSE provides an integrated measure of overall positioning accuracy. These metrics were computed consistently for static and kinematic PPP solutions under both open-sky and forest-obstructed conditions to ensure comparability.

Convergence behavior was evaluated using the three-dimensional (3D) positioning error derived from the combined E, N, and U components. Convergence time was defined as the first epoch at which the minimum value of a 20-epoch moving average of the 3D positioning error was achieved. This criterion was applied uniformly across all observation sessions to assess the influence of

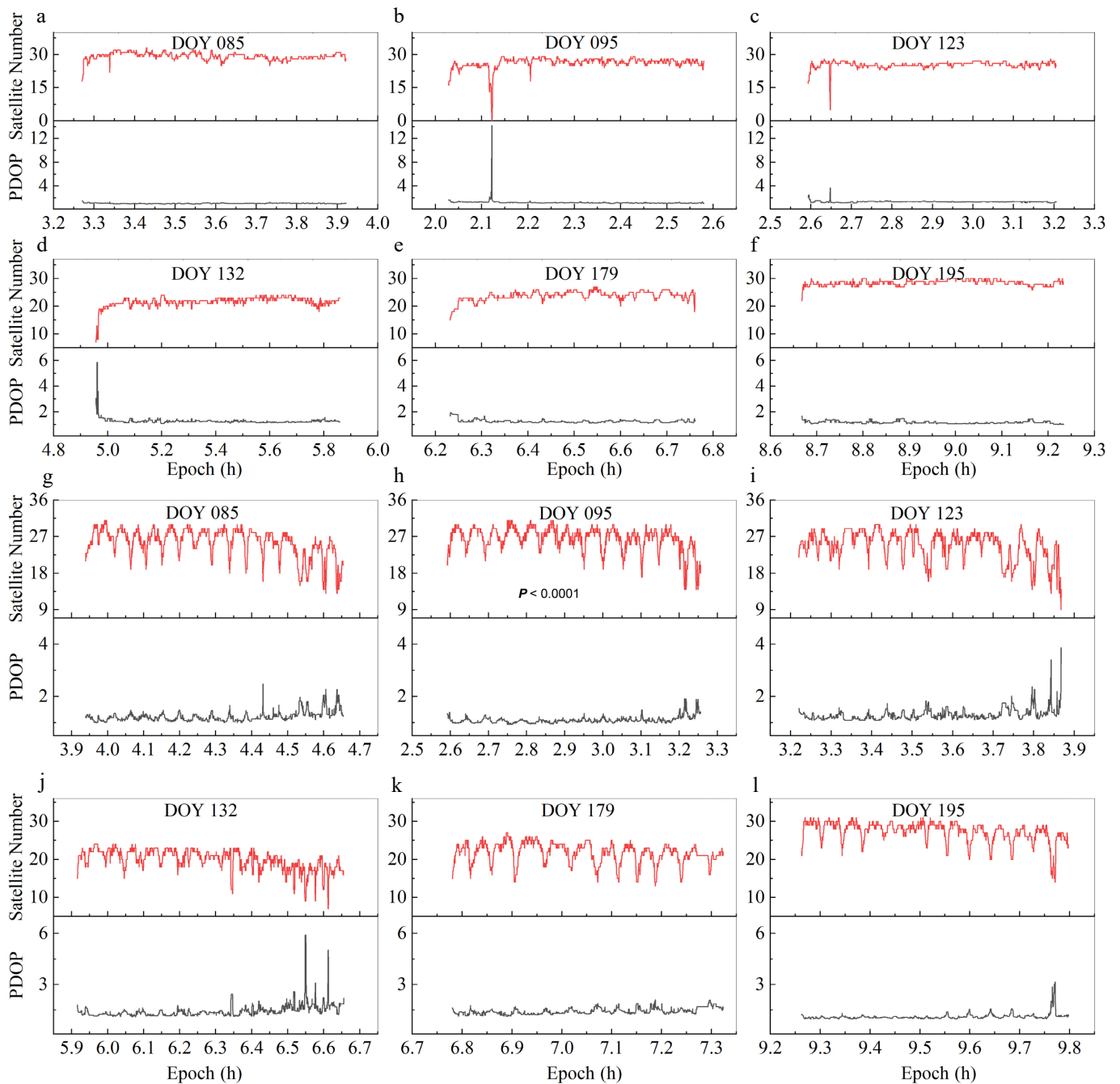


Fig. 3 Performance of satellite availability and PDOP under forest-obstructed environments across different observation days. (a)–(f) Static mode for DOY 085, 095, 123, 132, 179, and 195, respectively. (g)–(l) Kinematic mode for the corresponding DOY sequence.

environmental conditions and canopy density on PPP convergence characteristics.

All statistical analyses were conducted using identical processing strategies and evaluation criteria for different observation modes and experimental scenarios, ensuring objective and consistent performance comparison throughout the study.

Results

Positioning mode performance analysis

A statistical evaluation of multi-constellation PPP performance was conducted using representative observation periods selected at

approximately one-week intervals from DOY 078 to 195, 2023. Open-sky observations were first analyzed as a reference baseline to characterize the nominal performance of static and kinematic PPP under favorable satellite visibility, against which performance degradation under forest canopy conditions was subsequently evaluated.

Under open-sky conditions, multi-constellation PPP exhibits stable positioning performance in both static and kinematic modes, providing a reliable reference for subsequent analysis. Static PPP generally achieves higher accuracy than kinematic PPP across all coordinate components, particularly in the vertical direction, reflecting the benefits of long-term observation accumulation and favorable satellite geometry. Horizontal positioning accuracy remains at the decimeter level or better for both modes, indicating that satellite availability and observation redundancy are sufficient to support

Table 1. Precise Point Positioning and Double-Difference data processing models.

Category	Processing methods/strategies	
Data processing model	Double Difference	Precise Point Positioning
GNSS system	GPS/BDS/GLO/GAL	GPS/BDS/GLO/GAL
Observation type	Ionosphere-free (IF) model	Ionosphere-free (IF) model
Combination model	LC/PC ionospheric combination	LC/PC ionospheric combination
Stochastic model	Elevation angle	Elevation angle
Parameter estimation method	Kalman filtering	Kalman filtering
Orbit and clock offset	Broadcast ephemeris	Precise products
Coordinate frame	ITRF14	ITRF14
Antenna parameters of the receiver and satellite	igs14.atx (GPS parameters for the uncalibrated frequencies)	igs14.atx (GPS parameters for the uncalibrated frequencies)
Data sampling interval	1 s	1 s
Cut-off satellite elevation angle	10°	10°
Estimating parameter	Baseline vector	Position and clock offset

robust PPP solutions under unobstructed conditions (Fig. 4). In contrast, PPP performance deteriorates markedly under forest-obstructed environments, where canopy-induced signal attenuation and multipath effects fundamentally alter observation quality and satellite geometry. These effects are particularly pronounced for static PPP solutions.

Forest-obstructed environments impose substantial constraints on PPP performance, particularly for static positioning. In static PPP mode, severe signal attenuation and frequent satellite blockages result in pronounced accuracy degradation, with mean deviations ranging from -4.52 to 3.23 m (E), -0.86 to 7.28 m (N), and -9.68 to 3.22 m (U). Corresponding STD values increase to 0.36 – 5.33 m, 0.34 – 3.04 m, and 0.70 – 7.73 m, while RMSE values reach 0.67 – 5.53 m (E), 0.53 – 7.81 m (N), and up to 10.35 m in the U direction. These results indicate substantial instability and bias, particularly in the vertical component.

By comparison, kinematic PPP exhibits comparatively improved robustness in forest-obstructed scenarios. Mean deviations are reduced to -0.60 to 0.96 m (E), -1.22 to 1.82 m (N), and -2.77 to 3.14 m (U), with RMSE values ranging from 0.52 to 3.96 m, 0.78 to 5.22 m, and 2.20 to 7.54 m, respectively. Although significant fluctuations persist under severe obstruction—especially in the vertical direction—the kinematic mode provides more stable horizontal positioning and improved continuity relative to the static solution. These results are presented in Fig. 5.

Under forest-canopy conditions, the observed performance differences are primarily driven by environmental impacts on GNSS observation quality and satellite geometry. Forest canopy obstruction sharply reduces the number of visible satellites, increases PDOP values, and amplifies multipath effects due to the dominance of low-elevation signals. Frequent signal interruptions, cycle slips, and degraded carrier-phase observability further impair solution continuity, with the vertical component being the most vulnerable. Despite these challenges, kinematic PPP benefits from receiver mobility, which enhances geometric diversity and enables filtering algorithms—such as Kalman filtering—to exploit temporal correlations between epochs. This dynamic estimation framework improves resilience to short-term signal blockages and supports trajectory continuity, thereby partially mitigating the adverse effects of environmental obstruction. The asymmetric degradation among the E, N, and U components reflects the directional dependency of canopy-induced signal blockage, with the vertical (U) component being most vulnerable due to preferential obstruction of high-elevation satellites.

Analysis of the impact of forested and open scenarios on positioning performance

Under forest canopy conditions, environmental obstruction exerts a decisive influence on the convergence behavior and positioning accuracy of PPP solutions. Comparisons with open-sky reference scenarios are used to illustrate the magnitude of canopy-induced degradation in convergence efficiency, geometric stability, and achievable accuracy.

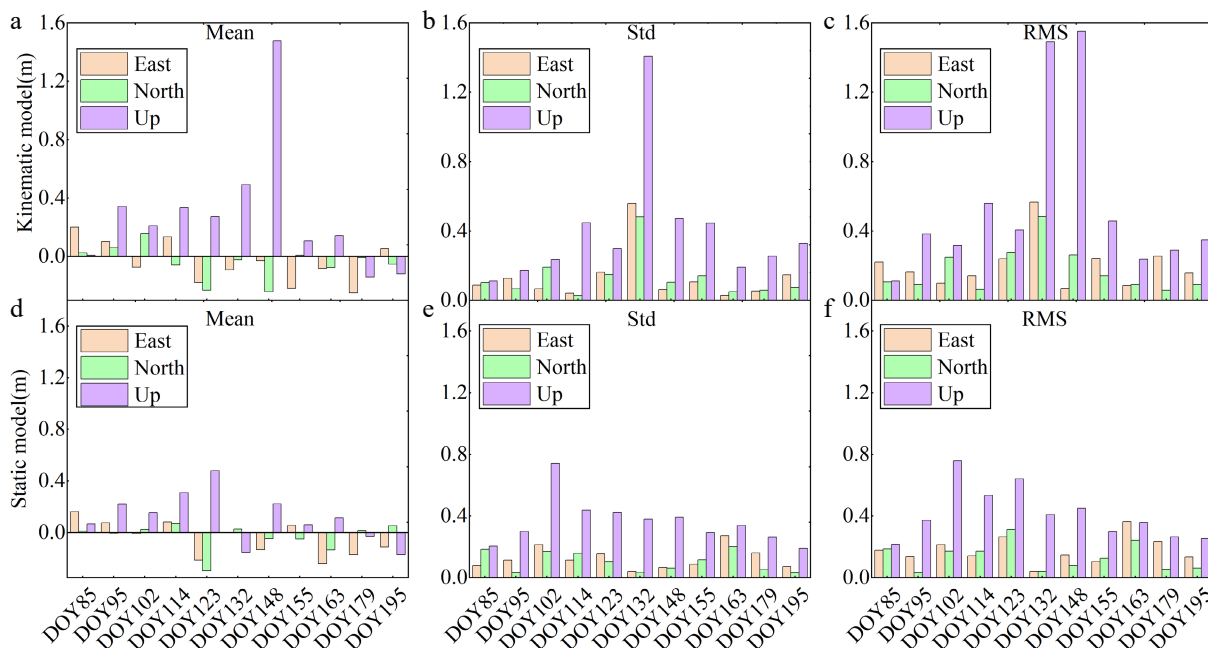


Fig. 4 Comparative statistical analysis of PPP positioning accuracy in open-sky scenarios (reference baseline). (a)–(c) Mean deviation, standard deviation (STD), and root mean square error (RMSE) for the kinematic mode. (d)–(f) Mean deviation, STD, and RMSE for the static mode.

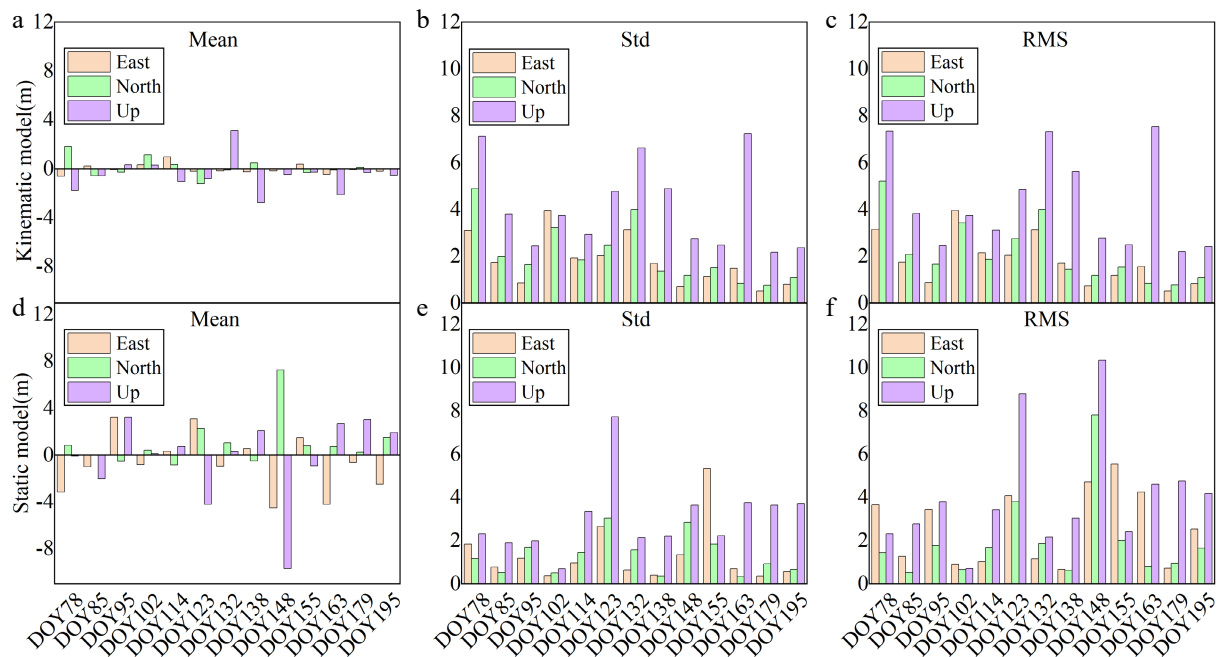


Fig. 5 Comparative statistical analysis of PPP positioning accuracy in forest-obstructed environments. (a)–(c) Mean, STD, and RMSE for the kinematic mode. (d)–(f) Mean, STD, and RMSE for the static mode.

Under open-sky reference conditions, static PPP exhibits rapid and stable convergence within approximately 6–10 min, supported by high satellite availability (25–35 satellites) and low PDOP values (1–2), providing an upper-bound benchmark for PPP performance. Under forest-obstructed conditions, PPP convergence is substantially prolonged, typically exceeding 15–20 min and, in some cases, failing to fully stabilize within the observation window. These delays coincide with frequent satellite blockages, abrupt reductions in satellite count, and pronounced PDOP fluctuations, reflecting persistent degradation of geometric strength (Fig. 6).

In forest-obstructed environments, static PPP positioning performance deteriorates markedly. Mean deviations increase to -0.70 m (E), 1.01 m (N), and -0.21 m (U), while RMSE values rise to 2.61 m, 1.97 m, and 4.10 m, respectively, indicating a transition from centimeter-level accuracy to decimeter- or meter-level accuracy under canopy obstruction, with the vertical component being most severely affected. The pronounced degradation of the vertical component can be primarily attributed to the geometric characteristics of the forest canopy and their impact on satellite visibility. Forest canopies predominantly obstruct signals from high-elevation satellites, which are critical for accurately resolving the height component in PPP solutions. As a result, the positioning solution becomes increasingly dependent on low-elevation satellites. These signals are more susceptible to residual tropospheric delay errors and multipath effects, both of which disproportionately propagate into the vertical component. In contrast, horizontal positioning can still be partially constrained by satellites distributed across different azimuths. However, the limited spatial extent of the measurement plot may also contribute to horizontal errors by restricting geometric diversity. For reference, under open-sky conditions, static PPP achieves centimeter-level accuracy with RMSE values below 0.5 m in all components (Fig. 7).

These results demonstrate that satellite visibility and geometric quality are the primary determinants of PPP performance. While static PPP performs robustly in open environments, forest obstruction significantly limits convergence speed and attainable accuracy due to reduced satellite availability, unfavorable elevation angle

distributions, intensified multipath effects, and frequent signal interruptions. Consequently, environmental conditions must be explicitly considered when applying PPP-based positioning in real-world scenarios characterized by severe signal obstruction.

Under forest-obstructed conditions, the positioning performance of kinematic PPP deteriorates markedly, consistent with the behavior observed for static PPP. In open-sky scenarios, kinematic PPP achieves relatively stable positioning accuracy, with mean deviations of -0.04 m (E), -0.04 m (N), and 0.29 m (U). The corresponding standard deviations are 0.13 m, 0.13 m, and 0.40 m, and the RMSE values are 0.20 m, 0.17 m, and 0.56 m in the E, N, and U directions, respectively.

In forest-obstructed environments, kinematic PPP performance degrades substantially. Mean deviations change to -0.02 m (E), 0.10 m (N), and -0.53 m (U), while standard deviations increase to 1.77 m, 2.07 m, and 4.10 m. Consequently, the RMSE values rise to 1.82 m, 2.15 m, and 4.29 m in the E, N, and U directions. The statistical results are shown in Fig. 8.

Influence of canopy density on positioning performance

Forest canopy density exerts a direct control on GNSS signal availability and, consequently, on PPP positioning performance. To quantify this influence, long-term time-series PPP solutions collected from DOY 078 to 195 in 2023 were analyzed under varying degrees of canopy closure. Both static and kinematic PPP solutions were evaluated with respect to convergence behavior and 3D positioning accuracy. For each epoch, PPP-derived position coordinates were compared with reference coordinates to compute 3D positioning errors. Convergence time was defined as the first epoch at which the minimum 20-epoch moving average of the 3D positioning error was achieved. Although direct measurements of leaf area index (LAI) were not available in this study due to logistical constraints associated with repeated *in situ* forest measurements over a long-term observation period, canopy density was indirectly characterized using satellite visibility and PDOP variations. These indicators have

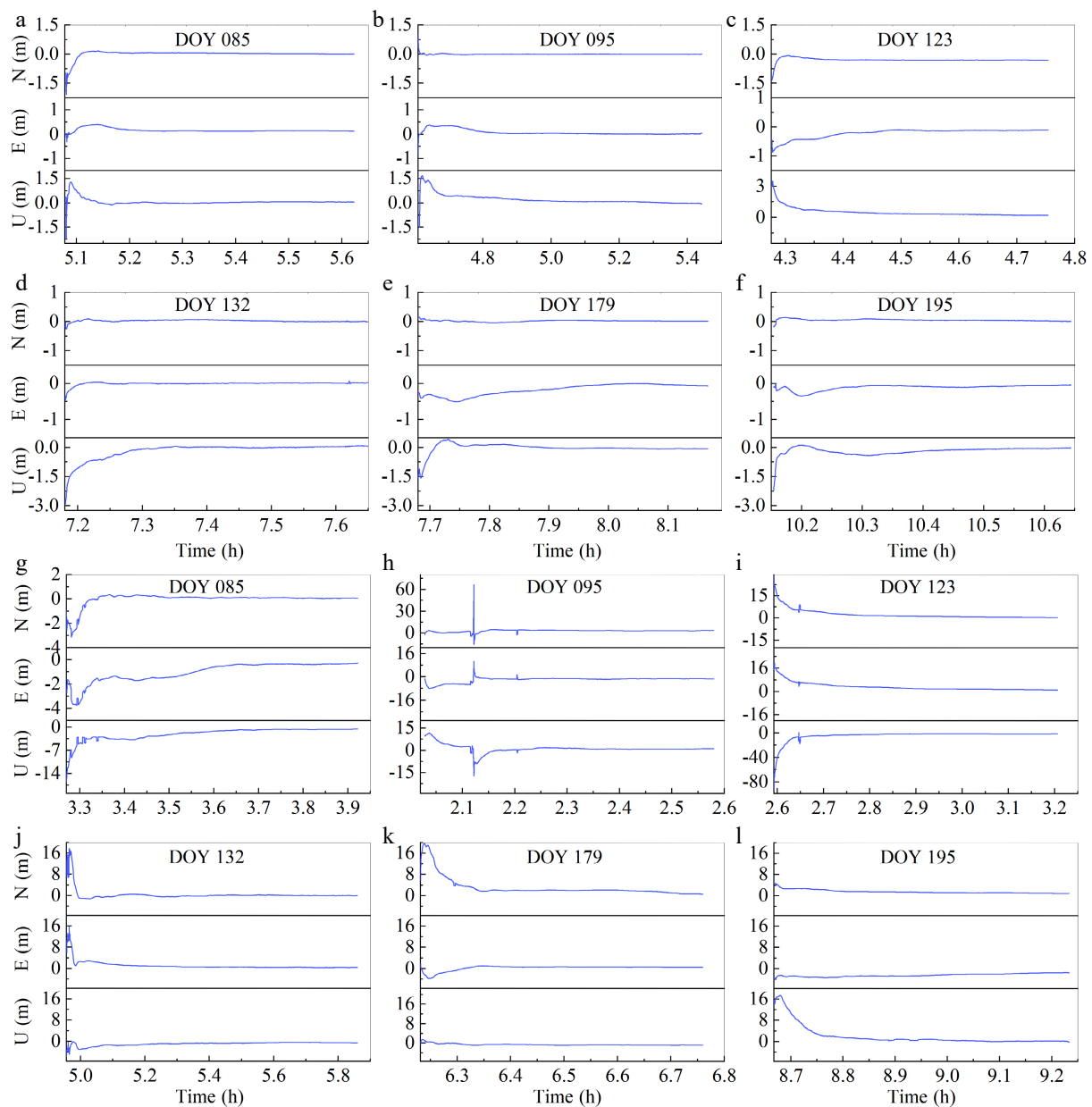


Fig. 6 Convergence behavior of static PPP under varying experimental scenarios. (a)–(f) Time-to-convergence in open-sky scenarios for DOY 085, 095, 123, 132, 179, and 195, respectively. (g)–(l) Corresponding convergence curves in forest-obstructed environments for the same DOY sequence.

been widely validated as effective proxies for canopy density and foliage dynamics in forested GNSS studies^[18,21].

Under canopy-obstructed conditions, static PPP generally exhibited a relatively stable number of tracked satellites, with most samples maintaining approximately 24 visible satellites and limited short-term variability. Corresponding PDOP values remained comparatively low, indicating that static observations can preserve a nominally stable geometric configuration despite persistent canopy obstruction. In contrast, kinematic PPP showed pronounced temporal variability in satellite visibility, with satellite counts fluctuating between approximately 15 and 30. These variations were accompanied by substantial PDOP fluctuations, typically ranging from 1.5 to 6, reflecting rapidly changing geometric conditions induced by receiver motion and intermittent signal blockage beneath the forest canopy.

The impact of increasing canopy density on PPP performance is further reflected in convergence behavior and positioning accuracy.

Static PPP exhibited comparatively long convergence times, predominantly between 25 and 40 min, with convergence exceeding 40 min at sites characterized by dense canopy cover. As canopy closure increased, static PPP showed a clear tendency toward delayed convergence and, in some cases, unstable solutions. By comparison, kinematic PPP achieved shorter and more consistent convergence times, generally within 15 to 40 min across the full range of canopy conditions.

A similar contrast is observed in 3D positioning accuracy. Static PPP achieved low RMSE values under sparse canopy conditions, but experienced pronounced accuracy degradation with increasing canopy density, with RMSE values reaching up to 6.34 and 4.03 m in heavily obstructed sites. In contrast, kinematic PPP maintained a narrower RMSE range throughout the observation period, with values between 0.26 and 1.13 m, indicating greater stability under varying canopy conditions. These results are summarized in Fig. 9.

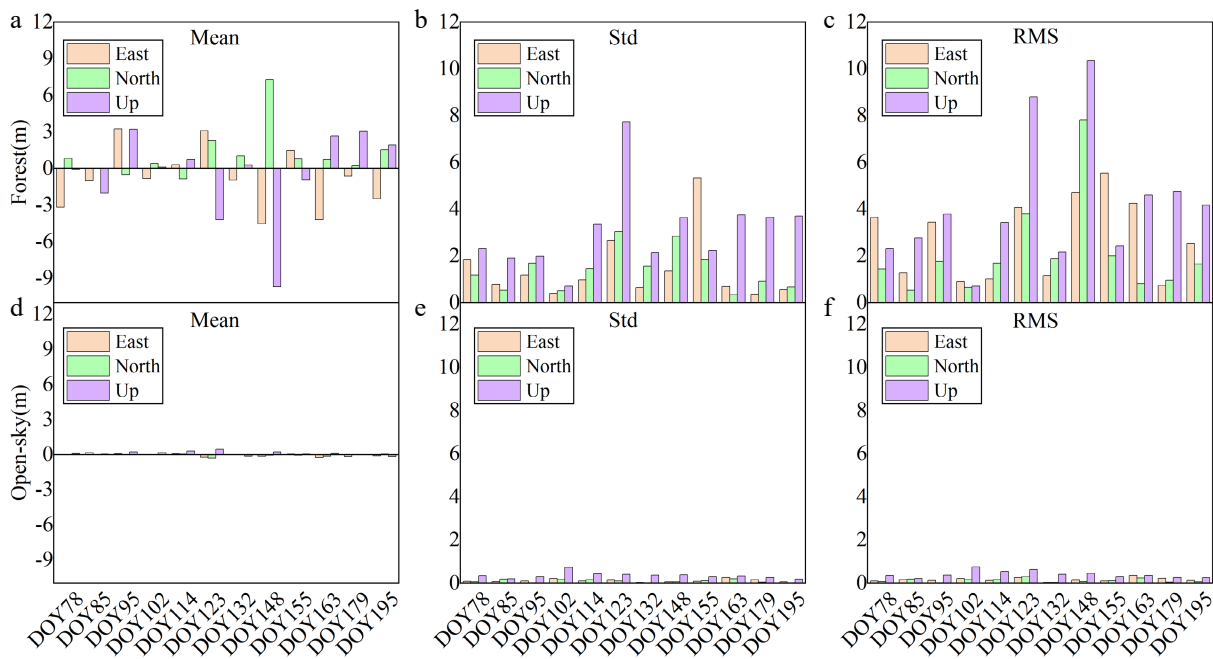


Fig. 7 Statistical accuracy comparison of static PPP between forest-obstructed and open-sky scenarios. (a)–(c) Mean deviation, standard deviation (STD), and root mean square error (RMSE) in forest-obstructed environments. (d)–(f) Mean deviation, STD, and RMSE in open-sky scenarios.

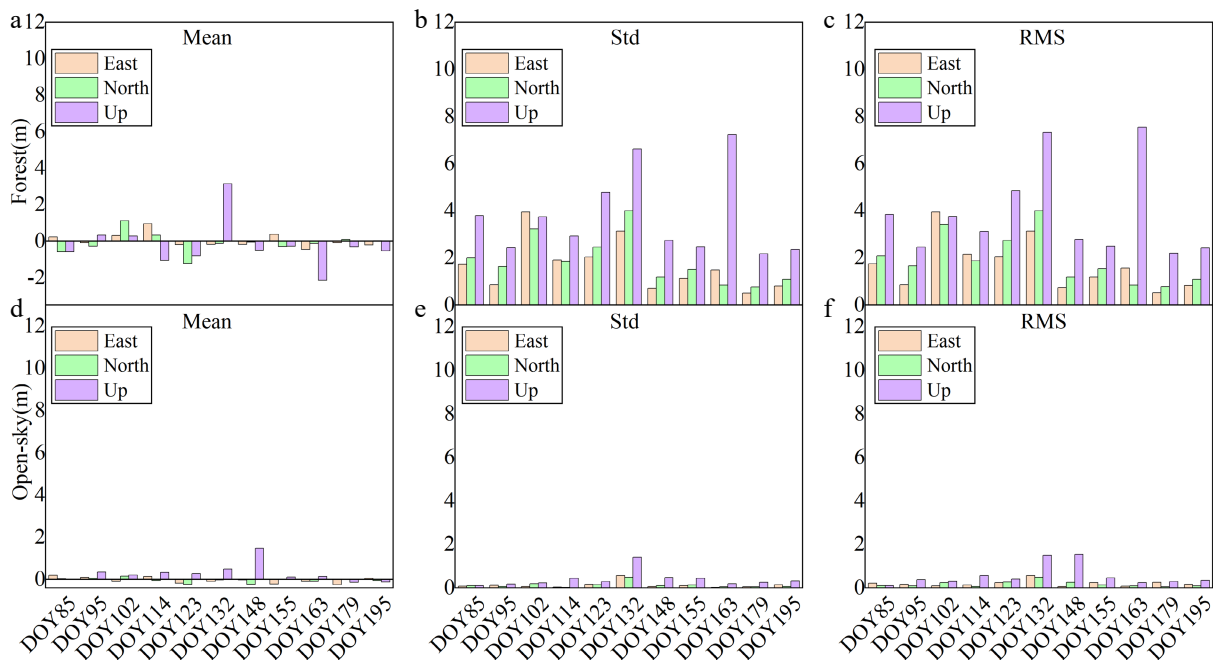


Fig. 8 Statistical accuracy comparison of kinematic PPP between forest-obstructed and open-sky scenarios. (a)–(c) Mean deviation, standard deviation (STD), and root mean square error (RMSE) in forest-obstructed environments. (d)–(f) Mean deviation, STD, and RMSE in open-sky scenarios.

Discussion

From a mechanistic perspective, PPP performance under forest canopy is primarily governed by satellite geometry degradation, increased observation noise, and mode-dependent estimation strategies. This study provides a comprehensive quantitative evaluation of PPP performance under varying environmental conditions and observation modes, and places these findings within the context of existing PPP studies to clarify when and why static or kinematic PPP may fail or succeed in forested environments.

Consistent with earlier studies^[3,22], open-sky environments remain the most favorable operational conditions for PPP. Under

such scenarios, static PPP benefits from stable satellite visibility and favorable geometric configurations, enabling rapid convergence and high positioning accuracy. However, the present results demonstrate that this advantage diminishes substantially under forest canopy conditions. As canopy density increases, static PPP exhibits pronounced degradation in both convergence behavior and positioning accuracy, particularly in the vertical component. While multipath interference and signal attenuation under vegetation have been widely reported^[18,19], most previous studies relied on short-term or single-epoch observations. In contrast, the long-term dataset analyzed here reveals a nonlinear degradation pattern, indicating the existence of a canopy-density threshold beyond which

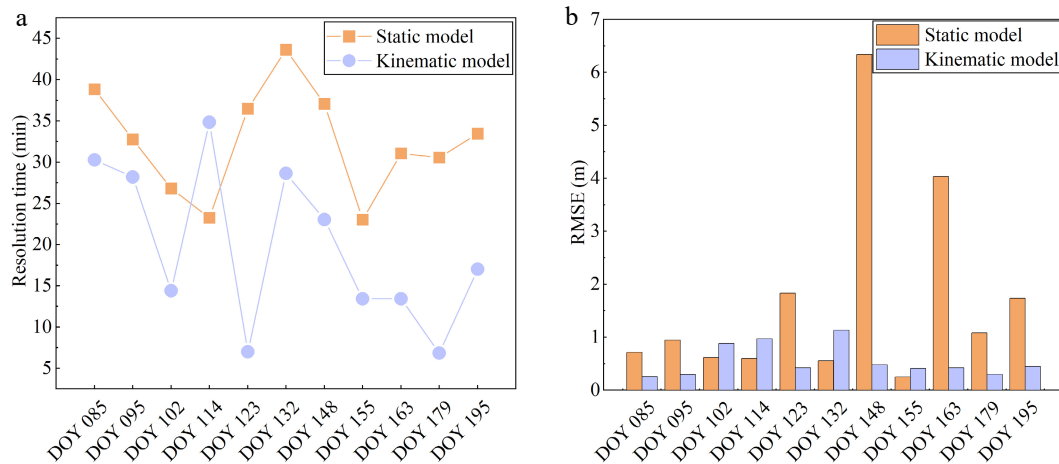


Fig. 9 (a) PPP convergence time statistics, and (b) 3D RMSE statistics.

static PPP frequently fails to converge reliably. The identified canopy-density threshold corresponds to a critical transition in satellite geometry and parameter estimability rather than a gradual degradation process. As canopy density increases, satellite visibility decreases, and PDOP rises progressively; however, once satellite availability falls below a critical level and PDOP exceeds a tolerable range, the PPP system undergoes a geometric breakdown. Under this condition, the normal equations become increasingly ill-conditioned, leading to a sharp reduction in ambiguity estimation reliability and convergence stability. This transition is clearly reflected by the abrupt increase in convergence time and RMSE shown in Fig. 9, which coincides with pronounced drops in satellite visibility and elevated PDOP values observed in Figs 2 and 3. These results indicate that the canopy-density threshold marks a shift from geometry-limited positioning to observation-noise-dominated PPP solutions, in which residual atmospheric errors and multipath effects dominate error propagation.

A central contribution of this study lies in the systematic comparison between static and kinematic PPP under varying canopy conditions. Receiver motion introduces motion-induced geometric diversity by continuously altering the relative geometry between the receiver and visible satellites. Even under partial signal blockage, this temporal change in geometry improves parameter observability compared with a static configuration. Within the Kalman filtering framework, this geometric diversity enables the state estimator to bridge short signal interruptions through temporal prediction and measurement updating, thereby mitigating the impact of intermittent satellite loss and enhancing solution continuity. This effect is indirectly reflected in the narrower RMSE range and more stable convergence behavior observed for kinematic PPP under dense canopy conditions. Contrary to the conventional assumption that static PPP is universally superior, the results show that kinematic PPP demonstrates greater robustness in forested environments. These observations are consistent with motion-enhanced robustness reported^[21,24], but the present results further demonstrate that trajectory continuity and temporal redundancy can outweigh the benefits of static observation stability under dense canopy conditions. This behavior can be primarily attributed to the geometric structure of forest canopies, which preferentially obstruct high-elevation satellite signals that are essential for resolving the vertical component. As a result, PPP solutions under dense canopy conditions rely more heavily on low-elevation observations, which are more susceptible to residual tropospheric delays and multipath effects. In contrast, horizontal positioning benefits from a wider

azimuthal distribution of satellites and is therefore relatively less sensitive to canopy-induced signal blockage. This finding provides empirical support for the hypothesis that kinematic PPP may represent a more suitable positioning strategy in highly obstructed natural environments.

The vertical component exhibits substantially greater degradation than the horizontal components in both observation modes. This anisotropic error behavior is primarily attributable to the preferential blockage of high-elevation satellites by the forest canopy, which weakens vertical geometric strength more severely than horizontal geometry; in dense beech plantations, broad leaves and continuous crown structures further exacerbate this effect by reducing near-zenith sky visibility and forcing the solution to rely on low-elevation signals that are more susceptible to multipath and atmospheric residuals. Compared with coniferous or mixed forests reported in previous studies^[8,28], the vertical RMSE values observed in this beech plantation are generally higher, highlighting the influence of broadleaf canopy structure and higher canopy closure. While similar vertical error amplification has been reported in previous studies^[14], the present analysis demonstrates that this degradation intensifies with increasing canopy density and seasonal foliage development. The vertical RMSE values (4–10 m) observed under dense canopy conditions are comparable to those reported^[28], while exceeding those reported for mixed forests^[8], highlighting the role of canopy closure. This indicates that vertical PPP accuracy in forested environments is fundamentally constrained by canopy geometry, rather than processing strategy alone, and that vegetation phenology introduces a time-varying bias that must be considered in long-term applications.

The long-term observation strategy adopted in this study also highlights the seasonal dependency of PPP performance, a factor rarely addressed in short-duration experiments. From early spring to late summer, positioning accuracy and convergence stability exhibit clear temporal trends that mirror vegetation growth cycles. While seasonal noise in PPP time series has been previously noted^[8,10], the present results demonstrate that seasonal canopy dynamics affect both static and kinematic solutions, reinforcing the necessity of long-term monitoring when evaluating GNSS performance in dynamic forest ecosystems.

These findings have direct practical implications for GNSS users operating in forested environments. Static PPP remains appropriate for applications requiring high absolute accuracy under low-canopy or open conditions, provided sufficient observation time is available. However, under moderate to dense canopies, kinematic PPP offers

greater robustness and reliability, particularly for mobile platforms and time-constrained surveys. The observed sensitivity of vertical positioning further suggests that applications demanding high vertical accuracy should avoid sole reliance on PPP under dense canopy, or incorporate auxiliary sensors. Moreover, observation timing and trajectory design emerge as practical considerations, as reduced foliage conditions and continuous motion can significantly improve solution stability.

Finally, this study points toward several directions for future research. Incorporating quantitative canopy descriptors derived from LiDAR or optical remote sensing would allow a more explicit linkage between vegetation structure and GNSS signal degradation. In addition, hybrid positioning strategies integrating inertial sensors and canopy-aware stochastic modeling, as well as adaptive filtering or machine-learning-based approaches, may further enhance PPP robustness in severely obstructed and time-varying forest environments.

Although the experiments were conducted in an artificial beech plantation, the key mechanisms identified in this study—namely satellite geometry degradation, enhanced multipath effects, and the contrasting responses of static and kinematic PPP under canopy obstruction—are not specific to a single forest type. These mechanisms are expected to be relevant across different forest structures and climatic conditions, although their quantitative impacts may vary with canopy composition, closure, and phenology. Consequently, while the numerical results reported here are site-specific, the observed performance trends and mechanistic interpretations provide useful reference for PPP applications in other forested environments.

The limitations of this study should also be explicitly acknowledged. First, the experiments were conducted in an artificial beech plantation, and the results may not be directly generalizable to natural or coniferous forests with different canopy structures and species compositions. Second, all experiments were performed using a single receiver type (M68), and potential receiver-dependent effects on PPP convergence and positioning performance were not evaluated.

Future work will focus on extending the analysis to diverse forest types and incorporating quantitative canopy descriptors, such as LiDAR- or optical-derived leaf area index, to strengthen the linkage between vegetation structure and PPP performance.

Conclusions

This study presents a systematic and long-term quantitative assessment of Precise Point Positioning (PPP) performance under varying environmental conditions, integrating static and kinematic observation modes across open and forested scenarios with different canopy densities. Based on GNSS data collected over an extended observation period in 2023, the results demonstrate that PPP accuracy and convergence behavior are jointly controlled by environmental obstruction and observation strategy. Under open-sky conditions, static PPP achieves rapid convergence and centimeter-level accuracy due to favorable satellite geometry and high signal redundancy, whereas kinematic PPP consistently maintains sub-meter precision. In contrast, forested environments significantly degrade PPP performance, particularly for static solutions, where reduced satellite visibility, increased PDOP variability, and canopy-induced multipath effects lead to prolonged convergence times and pronounced vertical errors.

A key finding of this study is the nonlinear relationship between canopy density and PPP performance. As canopy closure increases, static PPP exhibits a sharp decline in both accuracy and solution

stability, with convergence times frequently exceeding 30–40 min and positioning errors reaching the meter level or resulting in solution failure under dense vegetation. By comparison, kinematic PPP demonstrates greater robustness in obstructed environments, benefiting from motion-induced geometric diversity and filtering continuity that help mitigate intermittent signal loss. This challenges the conventional assumption that static PPP is universally superior and highlights the conditional advantage of kinematic PPP in complex forested settings. Additionally, the vertical component is consistently more vulnerable than the horizontal components, underscoring the inherent sensitivity of height estimation to canopy-induced signal attenuation and limited elevation-angle diversity.

From a practical perspective, these results provide clear guidance for PPP deployment in forested and semi-forested environments. Static PPP is recommended primarily for open or low-canopy conditions where sufficient observation duration can be ensured, whereas kinematic PPP is better suited for environments with moderate to high canopy density, especially for mobile platforms or time-constrained surveys. Applications requiring high vertical accuracy should be approached with caution under dense canopy conditions unless extended observation periods or auxiliary sensors are employed. These findings are particularly relevant for forestry surveying, ecological monitoring, and agricultural applications, where environmental obstruction is unavoidable and positioning reliability is critical.

Future research should focus on incorporating quantitative canopy descriptors derived from LiDAR or optical remote sensing into PPP stochastic modeling, as well as developing hybrid positioning frameworks that integrate PPP with inertial sensors or adaptive filtering strategies. In addition, canopy-aware observation weighting and seasonally adaptive error models represent promising directions for improving PPP robustness in dynamic vegetated environments.

Author contributions

The authors confirm contribution to the paper as follows: study conception and design, manuscript review and editing: Liu J; data collection, methodology and data processing, visualization and figure preparation, draft manuscript preparation: Zhang Y; analysis and interpretation of results: Zhang Y, Liu J. All authors reviewed the results and approved the final version of the manuscript.

Data availability

The dataset supporting the findings of this study, including raw GNSS observations, PPP processing scripts, and DD reference solutions, is available from the corresponding author upon reasonable request and completion of a data use agreement.

Acknowledgments

The authors would like to extend their sincere gratitude to all individuals and organizations who contributed to this research. First and foremost, we acknowledge the financial support provided by the Key Research and Development Program of Shaanxi (Grant Nos 2025NC-YBXM-209 and 2025NC-YBXM-210) and the National Natural Science Foundation of China (Grant Nos 32001249 and 32371875). We are profoundly grateful to the International GNSS Service (IGS) community for providing open access to their invaluable GNSS datasets, which formed the essential foundation for our analysis. Special thanks are extended to Yangling Huiqin Surveying and Mapping Co., Ltd and Shaanxi Zeling Information Technology

Co., Ltd for their strong technical and logistical support during the supplementary data collection campaigns. Finally, we are also indebted to the anonymous reviewers for their thoughtful comments and suggestions, which have greatly improved the quality of this manuscript.

Conflict of interest

The authors declare that they have no conflict of interest.

Dates

Received 31 December 2025; Revised 2 February 2026; Accepted 11 February 2026; Published online 30 March 2026

References

- Geng J, Shi C, Ge M, Dodson AH, Lou Y, et al. 2012. Improving the estimation of fractional-cycle biases for ambiguity resolution in precise point positioning. *Journal of Geodesy* 86:579–589
- Li T, Zhang H, Gao Z, Chen Q, Niu X. 2018. High-accuracy positioning in urban environments using single-frequency multi-GNSS RTK/MEMS-IMU integration. *Remote Sensing* 10:205
- Bisnath S, Gao Y. 2009. Current state of precise point positioning and future prospects and limitations. In *Observing our Changing Earth*, ed. Sideris MG. Vol 133. Berlin: Springer. pp. 615–623 doi: [10.1007/978-3-540-85426-5_71](https://doi.org/10.1007/978-3-540-85426-5_71)
- Kouba J. 2009. *A guide to using International gnss service (igs) products*. Booth Street, OT, Canada. <http://acc.igs.org/UsingIGSProductsVer21.pdf>
- Ramachandran D, Din AHM, Ibrahim SA, Omar AH. 2019. Real-time precise point positioning (RT-PPP) for positioning and mapping. In *GCEC 2017*, ed. Pradhan B. Vol 9. Singapore: Springer. pp. 891–913 doi: [10.1007/978-981-10-8016-6_64](https://doi.org/10.1007/978-981-10-8016-6_64)
- Li F, Pan C, Li Q, Yang J, Gao J, et al. 2024. An ambiguity subset selection algorithm based on the variation of check factors for bds-3/bds-2/gps precise point positioning. *GPS solutions* 29:41
- Elsheikh M, Iqbal U, Noureldin A, Korenberg M. 2023. The implementation of precise point positioning (PPP): a comprehensive review. *Sensors* 23:8874
- Feng T, Chen S, Feng Z, Shen C, Tian Y. 2021. Effects of canopy and multi-epoch observations on single-point positioning errors of a GNSS in coniferous and broadleaved forests. *Remote Sensing* 13:2325
- Shi Y, Xu T, Li M, Wei K, Wang S, Wang D. 2024. Real-time precise orbit determination of low earth orbit satellites based on GPS and BDS-3 PPP B2b service. *Remote Sensing* 16:833
- Maciuk K, Värna I, Xu C. 2021. Characteristics of seasonal variations and noises of the daily double-difference and PPP solutions. *Journal of Applied Geodesy* 15:61–73
- Abdelazeem M, Abazeed A, Kamal HA, Mohamed MOA. 2025. Ultra-low-cost real-time precise point positioning using different streams for precise positioning and precipitable water vapor retrieval estimates. *Algorithms* 18(4):198
- Li X, Huang J, Li X, Shen Z, Han J, et al. 2022. Review of PPP-RTK: achievements, challenges, and opportunities. *Satellite Navigation* 3:28
- Li X, Li X, Huang J, Shen Z, Wang B, et al. 2021. Improving PPP-RTK in urban environment by tightly coupled integration of gnss and ins. *Journal of Geodesy* 95:132
- Mohamed Safith A W, De Silva L. 2022. The techniques and challenges of gps surveying for vertical alignments in high-rise buildings. *International Journal of Building Pathology and Adaptation* 40:587–607
- Li L, Nie W, Zong W, Xu T, Li M, et al. 2025. High-precision multi-source fusion navigation solutions for complex and dynamic urban environments. *Remote Sensing* 17:1371
- Su K, Jin S, Hoque MM. 2019. Evaluation of ionospheric delay effects on multi-GNSS positioning performance. *Remote Sensing* 11:171
- Xiao Z, Sun S, Liu Z, Xu L, Huang W, et al. 2023. Propagation path loss models in forest scenario at 605 MHz. *Proc. 2022 IEEE 96th Vehicular Technology Conference (VTC2022-Fall), London, 2022*. US: IEEE. pp. 1–5 doi: [10.1109/VTC2022-Fall57202.2022.10012806](https://doi.org/10.1109/VTC2022-Fall57202.2022.10012806)
- Sawaguchi I, Saitoh Y, Tatsukawa S. 2005. A study of the effects of stems and canopies on the signal to noise ratio of GPS signals. *Journal of Forest Research* 10:395–401
- Pirtti A, Uçar Z, Kurtulgu Z, Eren M. 2025. Accuracy of global navigation satellite system (GNSS) positioning under tree canopy: evaluating the effect of extended antenna height and multiple GNSS systems. *Journal of the Indian Society of Remote Sensing* 53:3461–3474
- Brach M. 2022. Rapid static positioning using a four system GNSS receivers in the forest environment. *Forests* 13:45
- Kaartinen H, Hyypä J, Vastaranta M, Kukko A, Jaakkola A, et al. 2015. Accuracy of kinematic positioning using Global Satellite Navigation Systems under forest canopies. *Forests* 6:3218–3236
- Bu J, Yu K, Qian N, Zuo X, Chang J. 2021. Performance assessment of positioning based on multi-frequency multi-GNSS observations: signal quality, PPP and baseline solution. *IEEE Access* 2021:5845–5861
- Hu W, Uwineza J, Farrell JA. 2024. Outlier accommodation for gnss precise point positioning using risk-averse state estimation. *Proc. 2024 American Control Conference (ACC), 10–12 July, 2024, Toronto, ON, Canada*. pp. 1373–1379 doi: [10.23919/ACC60939.2024.10644650](https://doi.org/10.23919/ACC60939.2024.10644650)
- Xu X, Nie Z, Wang Z, Wang B, Du Q. 2022. Performance assessment of BDS-3 PPP-B2b/INS loosely coupled Integration. *Remote Sensing* 14:2957
- Hu W, Neupane A, Farrell JA. 2022. Using PPP information to implement a global real-time virtual network DGNSS approach. *Proc. IEEE Transactions on Vehicular Technology* 2022:10337–10349
- Li F, Psimoulis P, Li Q, Yang J, Gao J, et al. 2024. Assessment accuracy of standard point positioning enhanced by observation and position domain filtering utilizing a multi-epoch least-squares integration method. *Remote Sensing* 16(3):517
- Sun X, Shu Z, Yao J. 2025. Analyzing the precise point positioning performance of different dual-frequency Ionospheric-Free combinations with BDS-3 and galileo. *Atmosphere* 16(3):316
- Strunk J L, Reutebuch S E, McGaughey R J, Andersen H-E. 2025. An examination of gnss positioning under dense conifer forest canopy in the pacific northwest, USA. *Remote Sensing Applications: Society and Environment* 37:101428
- Abdi O, Uusitalo J, Pietarinen J, Lajunen A. 2022. Evaluation of forest features determining GNSS positioning accuracy of a novel low-cost, mobile RTK system using LiDAR and TreeNet. *Remote Sensing* 14:2856
- Hamza V, Stopar B, Sterle O, Pavlovčič-Prešeren P. 2024. Observations and positioning quality of low-cost GNSS receivers: a review. *GPS solutions* 28:149
- Rykała Ł, Rubiec A, Przybysz M, Krogul P, Ciešlik K, et al. 2023. Research on the positioning performance of GNSS with a low-cost choke ring antenna. *Applied Sciences* 13:1007
- Weaver SA, Ucar Z, Bettinger P, Merry K. 2015. How a gnss receiver is held may affect static horizontal position accuracy. *PLoS One* 10:e0124696
- Wing M G. 2011. Consumer-grade gps receiver measurement accuracy in varying forest conditions. *Research Journal of Forestry* 5:78–88
- Zimelman EG, Keefe RF. 2018. Real-time positioning in logging: effects of forest stand characteristics, topography, and line-of-sight obstructions on GNSS-RF transponder accuracy and radio signal propagation. *PLoS One* 13:e0191017
- Bakuła M, Oszczak S, Pelc-Mieczkowska R. 2009. Performance of RTK positioning in forest conditions: case study. *Journal of Surveying Engineering* 135:125–130
- Piedallu C, Gégout J-C. 2005. Effects of forest environment and survey protocol on GPS accuracy. *Photogrammetric Engineering & Remote Sensing* 71:1071–1078
- İlçi V. 2019. Accuracy comparison of real-time GNSS positioning solutions: case study of Mid-North Anatolia. *Measurement* 142:40–47



Copyright: © 2026 by the author(s). Published by Maximum Academic Press, Fayetteville, GA. This article is an open access article distributed under Creative Commons Attribution License (CC BY 4.0), visit <https://creativecommons.org/licenses/by/4.0/>.